

TLE5501

TMR-Based Angle Sensor

User's Manual

About this document

Scope and purpose

This document covers the TMR angle sensor TLE5501 with its versions E0001 and E0002.

Intended audience

This document is aimed at experienced hardware and software engineers using the TLE5501 angle sensor

Table of Contents

1	Application Circuits	3
2	Transient behavior	5
2.1	Bandwidth of the TMR bridge	5
2.2	Recommendation for the external capacitor C_b	9
3	Connection to a micro controller	10
3.1	Sigma-Delta ADC	10
3.2	SAR ADC	10
3.2.1	Load step	11
3.2.2	Load step reduction	13
3.2.3	Oversampling	14
4	Calibration	15
5	Revision History	18

Application Circuits

1 Application Circuits

The application circuits in this chapter show the various connection possibilities of the TLE5501. It can be used in a single ended mode (only one sine and one cosine signal, [Figure 1](#) and [Figure 3](#)) and in a differential mode with a total of four output signals ([Figure 2](#) and [Figure 4](#)).

To fully implement the safety concept of the TLE55001 E0002 version and achieve highest diagnostic coverage, the four output signals have to be sampled singled ended. This is necessary, as the proposed external safety mechanisms in the Safety Manual act on the single ended signals. Nevertheless, to reach highest angle accuracy, the differential calculated angle shall be used for the application. The single ended signals are for diagnostic only.

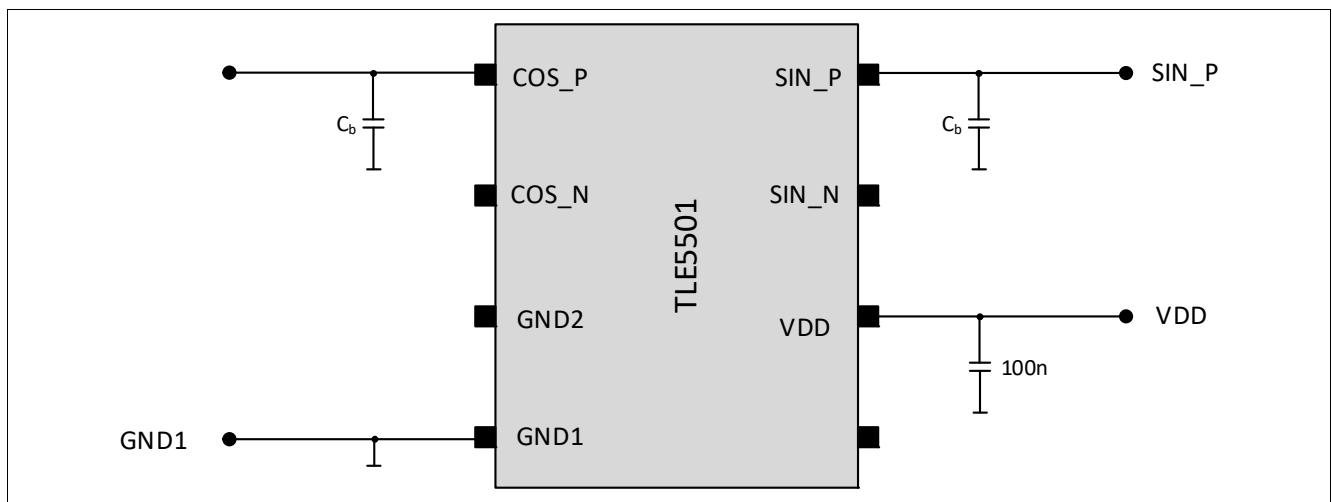


Figure 1 Application circuit for TLE5501 E0001 single ended signal used

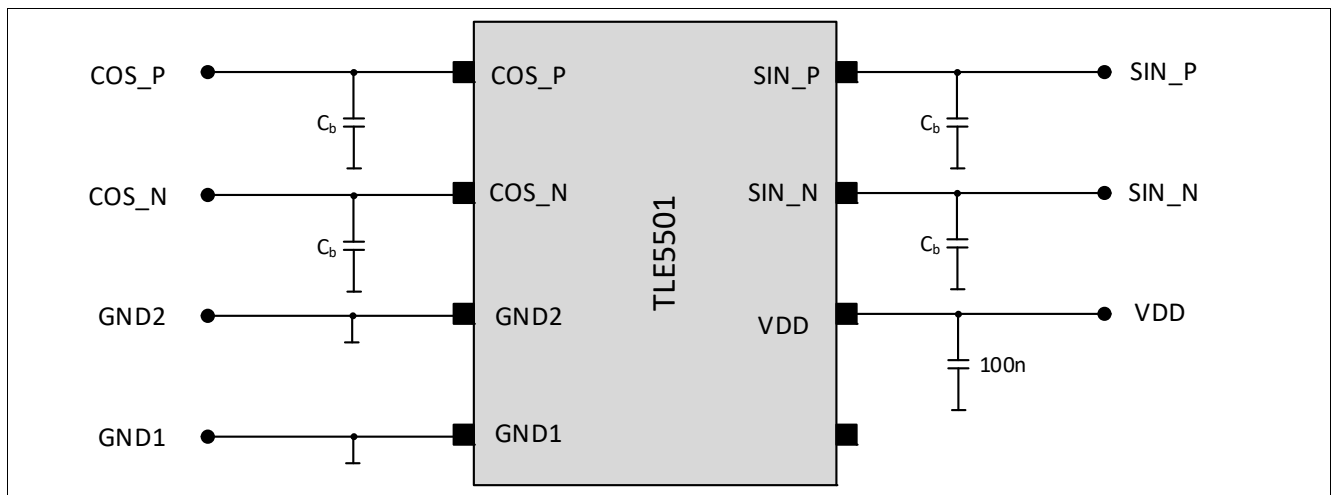


Figure 2 Application circuit for TLE5501 E0001 differential signal used

Application Circuits

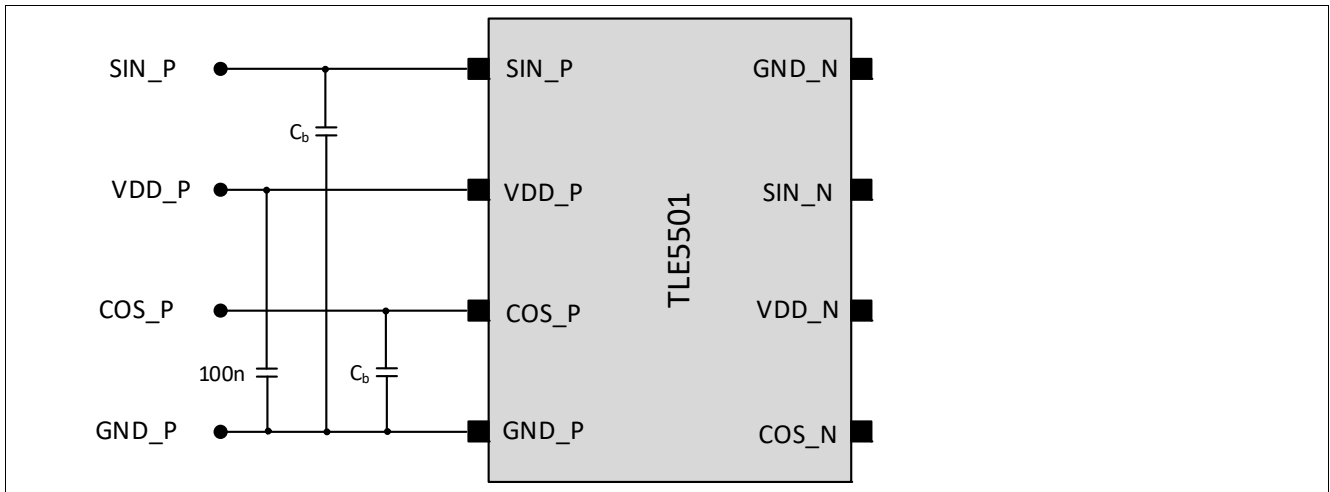


Figure 3 Application circuit for TLE5501 E0002 single ended signal used

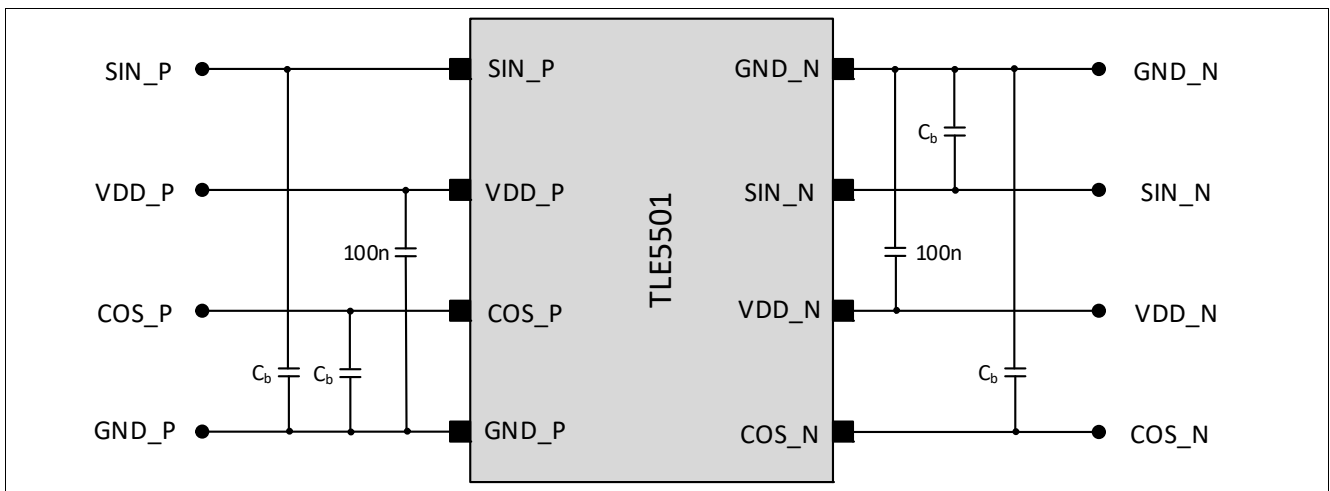


Figure 4 Application circuit for TLE5501 E0002 differential signal used

It is recommended to use a 100nF capacitor on the VDD pin to filter noise on the supply line. As the device is ratiometric, any noise on the supply is coupled to the sensor output.

2 Transient behavior

For the sine and cosine output pins, it is also recommended to use a buffer capacitor C_b for filtering purpose. As the device itself has a high output impedance, given by the TMR resistors R_{TMR} , this buffer capacitor builds a low-pass filter together with the bridge resistivity.

2.1 Bandwidth of the TMR bridge

It has to be taken into account that the low pass filter limits the bandwidth of the sensor and increases step response time. **Figure 5** shows a schematic of the sensor output structure with an external capacitor C_b . The resistivity of a TMR resistor R_{TMR} is specified in the datasheet and has a value between $4k\Omega$ and $8k\Omega$.

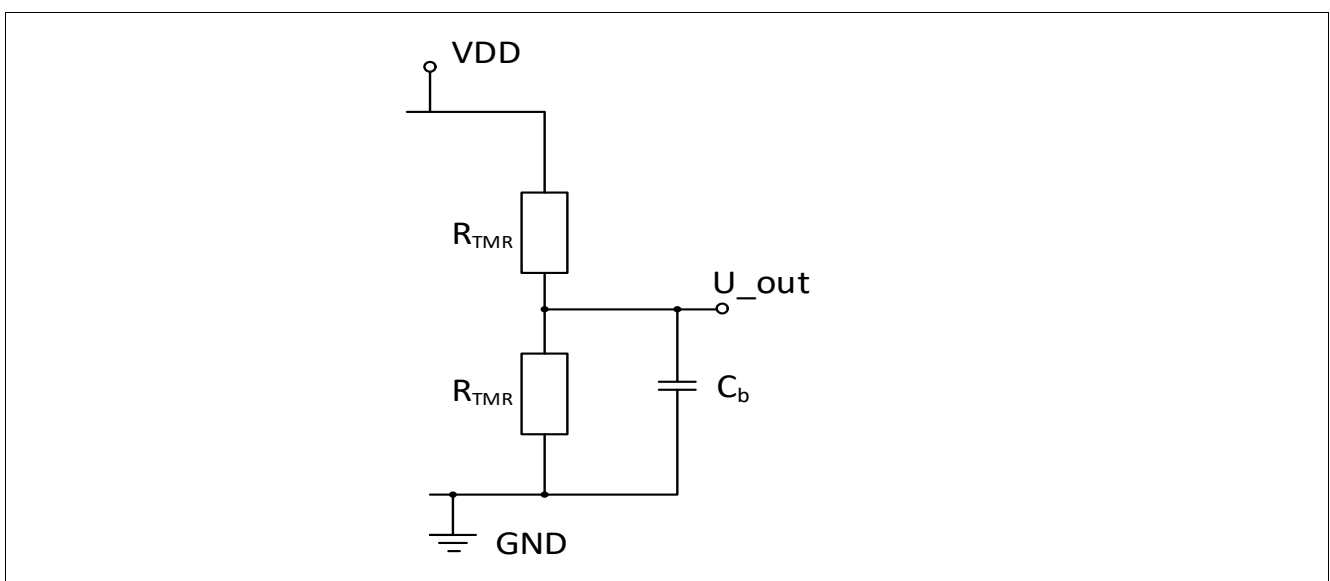


Figure 5 Schematic of one branch of the TMR bridge with external buffer capacitor C_b

The result of a pSPICE simulation of this output structure is shown in **Figure 6**. A resistor of $R_{TMR} = 8k\Omega$ and a capacitor value of $C_b = 1nF$ is assumed. Applying a voltage step of $5V$ on the supply V_{DD} is simulated. This is compared with analytical simulations using below **Equation (2.1)**:

(2.1)

$$U(t) = U_0(1 - e^{-t/\tau})$$

The time constant for the bridge τ_{br} is defined as: $\tau_{br} = RC$, U_0 is taken to be $2.5V = V_{DD}/2$.

A good approximation of the transient behavior in the analytical calculation can be achieved with $R = 4k\Omega$ and $C_b = 1nF$, so R in the analytical simulation is half of the resistivity of one TMR resistor R_{TMR} of the bridge.

This behavior is equal to a low-pass filter at the sensor output with $R = R_{TMR}/2$ and C_b .

Transient behavior

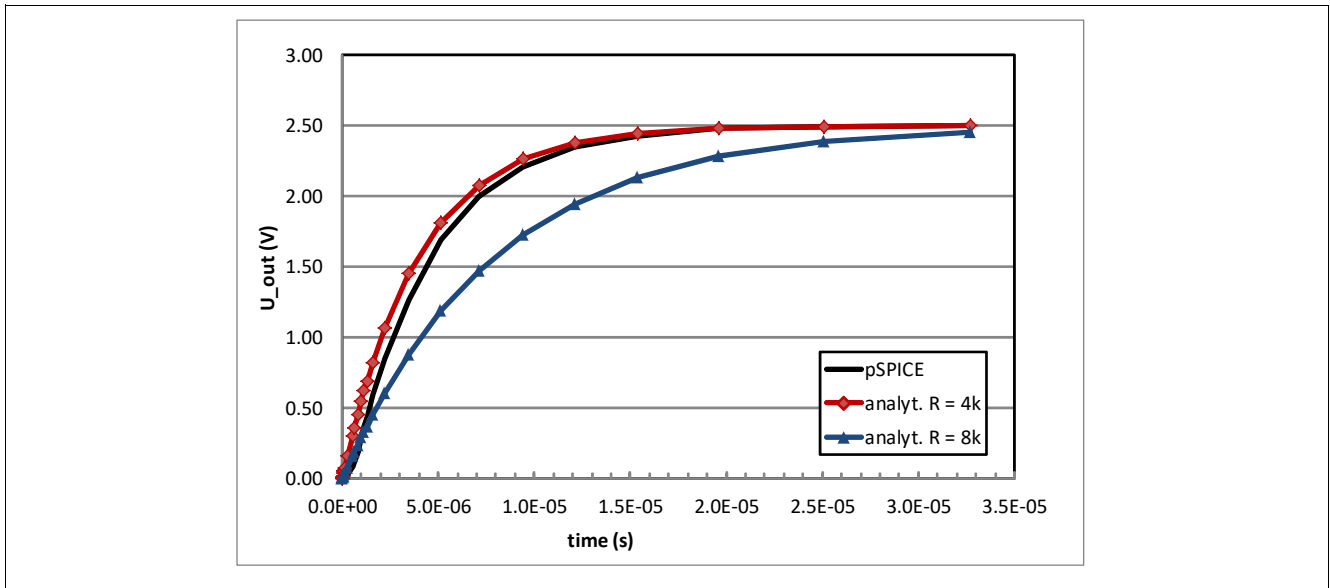


Figure 6 Simulation (pSPICE and analytical) of the RC behavior of the output voltage ($R_{TMR} = 8k\Omega$, $C_b = 1nF$). Voltage step on V_{DD} . The 100nF capacitor on V_{DD} is not included in the simulations

The transient behavior when applying an AC magnetic field with frequency f is shown in [Figure 7](#) and [Figure 8](#). The pSPICE simulation is compared with analytical calculations according to [Equation \(2.2\)](#) and [Equation \(2.3\)](#) below. Again, a good fit is achieved using $R = 4k\Omega$ for the calculation.

(2.2)

$$\frac{U(t)}{U_0} = \frac{X_c}{\sqrt{R^2 + X_c^2}}, X_c = \frac{1}{2\pi f \cdot C}$$

(2.3)

$$\text{Phase} = -\arctan(2\pi fRC)$$

Transient behavior

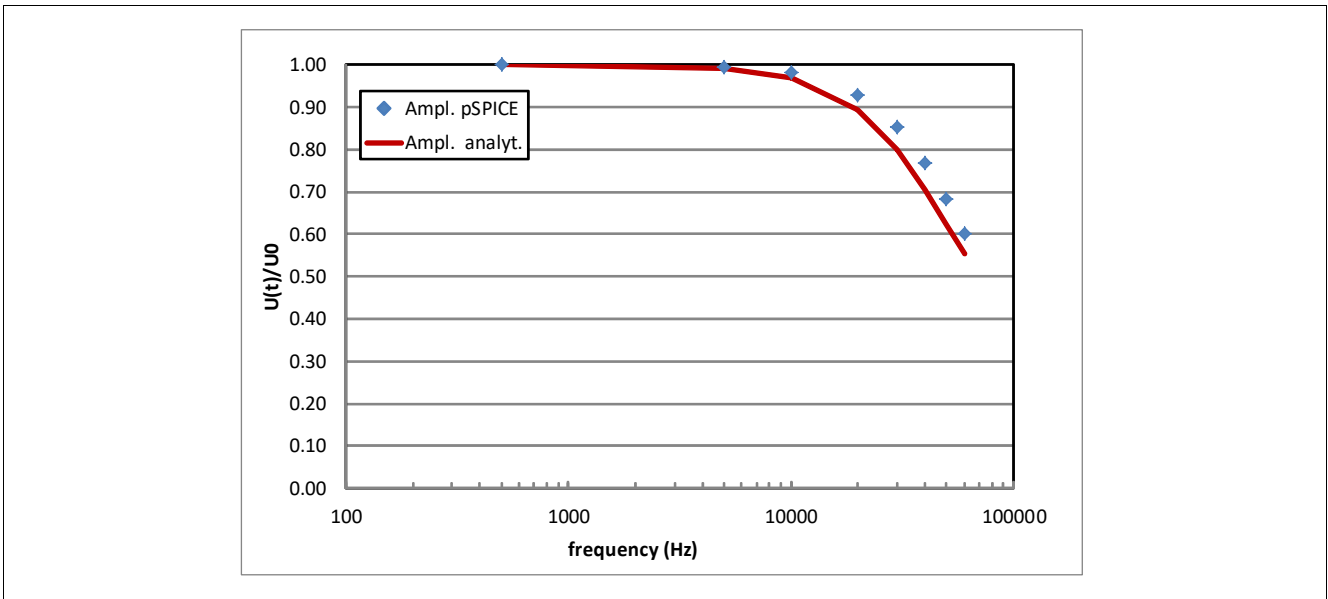


Figure 7 Normalized output amplitude for an AC magnetic field excitation. Bridge resistor $R_{TMR} = 8k\Omega$, $C_b = 1nF$. For the analytical calculation, the values $R = 4k\Omega$ and $C_b = 1nF$ are used (Equation (2.2))

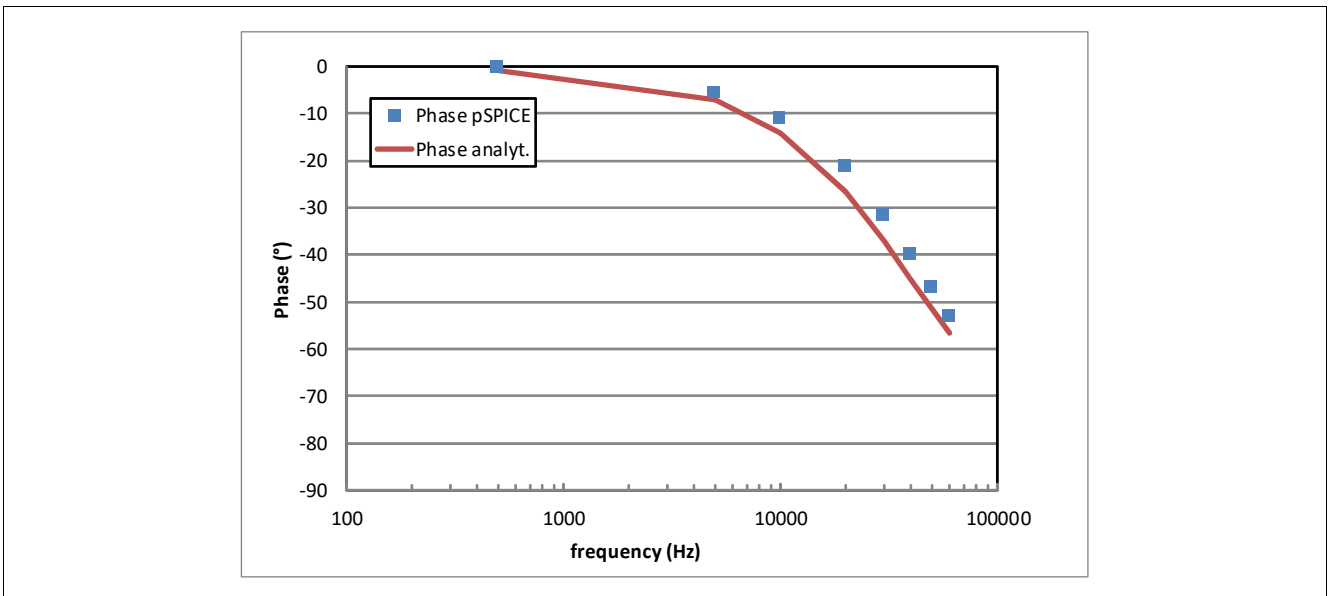


Figure 8 Phase shift between output signal and excitation for an AC magnetic field. Bridge resistor $R_{TMR} = 8k\Omega$, $C_b = 1nF$. For the analytical calculation, the values $R = 4k\Omega$ and $C_b = 1nF$ are used (Equation (2.3))

The transient behavior of the TMR output can be approximated with a simple RC model, using $R = R_{TMR}/2$.

Transient behavior

For a bridge resistivity of $R_{\text{TMR}} = 8\text{k}\Omega$ and a buffer capacitor of $C_b = 1\text{nF}$, the cut-off frequency f_c is calculated according to [Equation \(2.4\)](#) with $R = R_{\text{TMR}}/2$.

(2.4)

$$f_c = \frac{1}{2\pi RC} = \frac{1}{\pi R_{\text{TMR}} C} = 39.78\text{kHz}$$

Care should be taken, that the buffer capacitor C_b is chosen in a way that the phase shift between output signal and input signal does not impact the angle accuracy for the maximum given frequency in the application.

For example, to have the phase shift Φ below 0.2° with a $C_b = 1\text{nF}$, the maximum frequency f_{rotation} in the application is estimated according [Equation \(2.5\)](#) to be below $139\text{Hz} = 8340\text{rpm}$.

(2.5)

$$f = \frac{\tan(\Phi)}{2\pi RC}$$

As the TLE5501 is a passive sensor with analog output, also further capacitive load, coming e.g. from the ADC input of the microcontroller has to be considered. Further details to that are given in [Chapter 3](#). The operation of the TLE5501 should always be well below the calculated cut-off frequency f_c with the total capacitive load considered (buffer capacitor C_b , ADC input capacity, parasitics) and assuming a worst case bridge resistivity R_{TMR} according to the datasheet. Depending on the accuracy requirements of the application, it might be necessary to further reduce the input magnetic frequency to minimize the phase shift between input and output signal to the required value.

Settling time τ_s of a RC filter

Assuming an ADC with N bits resolution, which is used to measure the bridge output signal, it is desired that the measurement error of the output voltage is less than 0.5LSB .

To achieve this, the input frequency has to be low compared to the cut-off frequency f_c ([Equation \(2.4\)](#)), given by the RC time constant τ_{br} of the bridge resistivity and the external capacitor.

Using [Equation \(2.1\)](#), the following relation can be obtained for the time until the voltage reaches U_0 with a deviation of less than 0.5LSB :

(2.6)

$$U(t) = U_0 \cdot (1 - e^{-t/\tau}) = U_0 \cdot \left(1 - \frac{0.5}{2^N}\right)$$

Transient behavior

For the time τ_s until the voltage settles to a value less than 0.5LSB from final value U_0 the following relation holds:

(2.7)

$$\tau_s = -\left(\tau_{br} \cdot \ln\left(\frac{0.5}{2^N}\right)\right)$$

For a 12 bit ADC with $N = 12$, τ_s becomes $\tau_s = 9.0\tau_{br}$.

This means that a waiting time of approx. 9 times of τ_{br} should be considered for settling the signal before it can be converted with the ADC.

2.2 Recommendation for the external capacitor C_b

For most applications, it is a target to achieve a high angle accuracy. To reach this, the phase shift Φ between the magnetic input signal and the bridge output shall be small. It can be estimated using [Equation \(2.3\)](#).

The external buffer capacitor C_b can be calculated depending on magnetic input frequency f_{in} and desired phase shift Φ according to [Equation \(2.8\)](#):

(2.8)

$$C_b = \frac{\tan(\Phi)}{2\pi R f_{in}}$$

For an application with 8000rpm, $f_{in} = 133\text{Hz}$, $R = 4\text{k}\Omega$ ($R = R_{TMR}/2$, see [Chapter 2.1](#)) and $\Phi = 0.2^\circ$ the maximum buffer capacitor C_b is calculated to $C_b = 1\text{nF}$.

The time constant τ_{br} of the bridge in this case is $\tau_{br} = R_{TMR}/2 \times C_b = 4\text{k}\Omega \times 1\text{nF} = 4\mu\text{s}$.

So the settling time of the bridge τ_s is then $\tau_s = 9\tau_{br} = 36\mu\text{s}$.

For applications with higher speed, the buffer capacitor C_b can be further reduced but it has to be taken into account, that there is also a capacitive load of the ADC of the microcontroller which needs to be charged. Further details in [Chapter 3](#).

3 Connection to a micro controller

The following chapters give some hints which should be considered when the TLE5501 is connected to a microcontroller.

3.1 Sigma-Delta ADC

In a Sigma-Delta ADC, the analog input signal is converted into a bit stream with the bit density corresponding to the analog input value. The sampling frequency is much higher (~MHz) than the signal frequency. A decimation filter converts the bit stream into a digital word (demodulation).

This type of ADC has typically a high input resistivity which makes it ideally suited for connection to a high impedance current source. Very low input currents are drawn which do not influence the sensor output voltage. Also, high resolution can be achieved which, however, comes together with a larger delay of the signal.

Difficult for this type of ADC is the synchronization of the sine and cosine channel, which is mandatory to achieve a high angle accuracy. To implement the proposed safety mechanisms for the TLE5501, it is also required to sample the single ended signals SIN_P, SIN_N, COS_P, COS_N. This makes single ended ADC channels necessary. The four channels should be sampled synchronous or with a very low time difference.

If the microcontroller in use allows to implement the above described requirements, a Sigma-Delta ADC is a good choice for the connection to the TLE5501.

3.2 SAR ADC

The SAR (successive approximation register) is a widely used ADC and available on most micro controllers. Its input is a switched capacitor structure with a sample and hold circuit. It supports a fast sampling frequency with a typical resolution of 10 to 12 bits.

Figure 9 shows an input structure of an SAR ADC. In the “sample” phase, the S/H switch is closed and the “sample and hold” capacitor C_{SH} is charged via the resistor R_{SH} (sampling time). After the sampling time the switch S/H is opened and the voltage stored in C_{SH} is converted to a digital value (hold time). The total time required for charging the capacitor and conversion to a digital value is called conversion time.

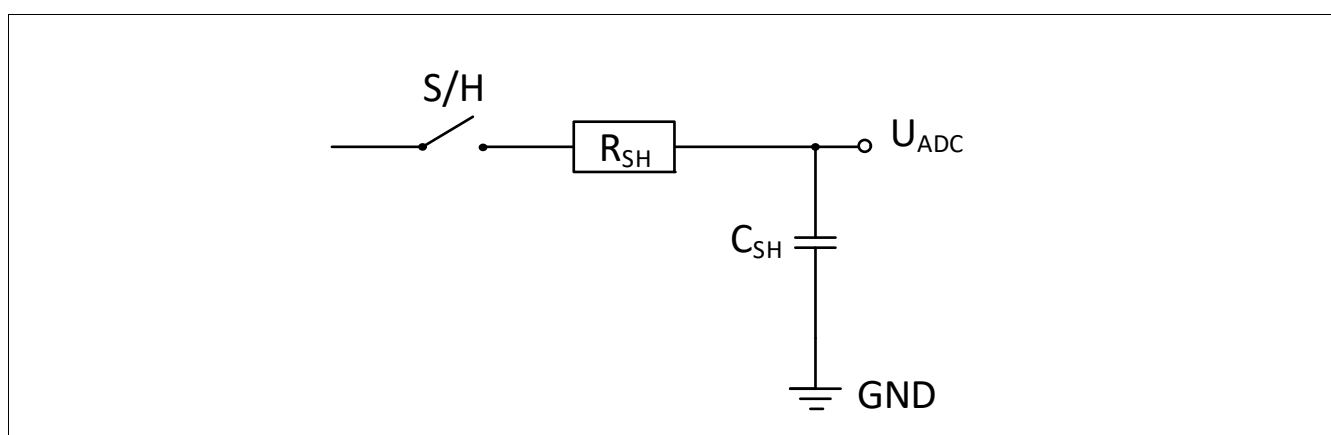


Figure 9 Schematic input structure of an SAR ADC.

The high output impedance of the TMR bridge together with the external buffer capacitor C_b has a considerable impact on the timing behavior of the SAR ADC. An equivalent circuit is shown in **Figure 10**.

Connection to a micro controller

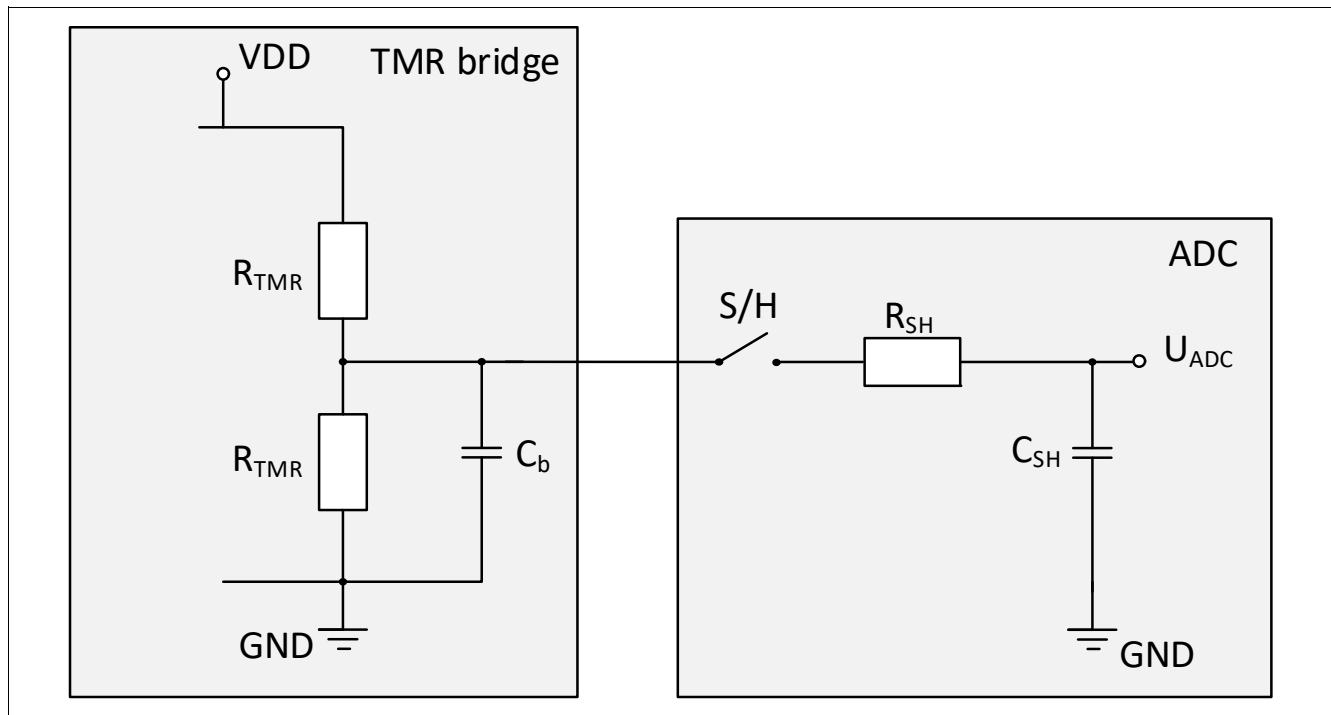


Figure 10 Equivalent circuit of TMR bridge (only half bridge is shown) and SAR ADC input

3.2.1 Load step

The following consideration is made with the initial condition that the buffer capacitor C_b is fully charged, the S/H switch is open and the sample and hold capacitor C_{SH} is discharged. In this condition, the voltage at C_b is $V_{DD}/2$ and the voltage $U_{ADC} = 0V$.

When the S/H switch is closed, charge is flowing from C_b to C_{SH} , the voltage at C_b drops and the voltage at C_{SH} , U_{ADC} , increases. In addition, charge is flowing from the supply voltage V_{DD} via the TMR resistor R_{TMR} to charge C_b .

The following parameters are assumed: $V_{DD} = 5V$, $R_{TMR} = 8k\Omega$, $C_b = 1nF$, $R_{SH} = 2k\Omega$, and $C_{SH} = 7pF$.

The time constant τ_{br} for charging C_b via R_{TMR} is given by $\tau_{br} = R_{TMR}/2 \times C_b = 4\mu s$ (see also [Chapter 2.2](#)).

For charging C_{SH} the time constant $\tau_{SH} = R_{SH} \times C_{SH} = 14ns$. Therefore, the charging of C_{SH} and also the de-charging of C_b is much faster ($\sim 9 \times 14ns = 140ns$) than the recovery of the voltage at C_b ($\sim 9 \times 4\mu s = 36\mu s$).

Due to this, with the assumption that $\tau_{br} \gg \tau_{SH}$ the voltage at C_b drops by a value of ΔU which can be approximated as follows ([Equation \(3.1\)](#)):

(3.1)

$$\Delta U = U_0 \frac{C_{SH}}{(C_b + C_{SH})}$$

With above parameters and $U_0 = 2.5V$, the load step is calculated to $\Delta U = 17.4mV$. The time constant τ_{br} of the bridge defines how long it takes until the voltage U_{ADC} is settled with sufficient accuracy (error less than 0.5LSB). Therefore, the sampling time (time for which S/H switch has to be closed) must be larger than $9 \times \tau_{br} = 9 \times 4\mu s = 36\mu s$.

[Figure 11](#) shows this behavior. At $t = 1\mu s$ the S/H switch is closed and remains so until $t = 37\mu s$. In the first moment, the voltage drops by $\Delta U = 17mV$ and then increases with the time constant of the bridge $\tau_{br} = 4\mu s$.

Connection to a micro controller

After 36µs the capacitors C_{SH} and C_b are almost fully charged, the S/H switch is opened and the ADC can start with the conversion and will sample the correct voltage of $V_{DD}/2$. After the hold time the capacitor C_{SH} is discharged and the next sampling phase starts.

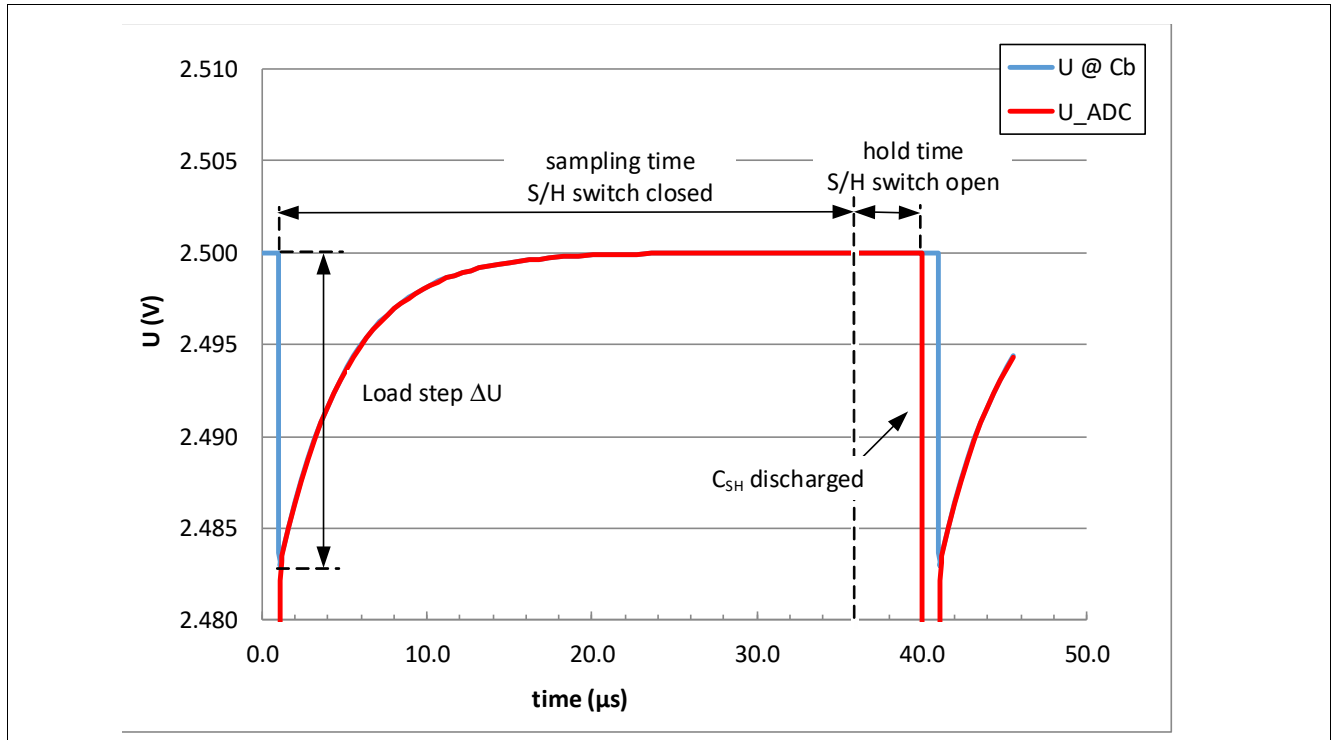


Figure 11 Sampling and conversion of the TMR bridge signal with a SAR ADC.

The time constant of the bridge $\tau_{br} = R_{TMR}/2 \times C_b$ is determining the maximum possible sampling frequency f_{sample} . In above example the maximum sampling frequency is estimated to $f_{sample} \sim 27.7\text{kHz}$ (**Equation (3.2)**) In reality, the achievable sampling frequency is lower, as also some additional time has to be included for the hold time of the ADC. Sampling time and hold time are depending on the settings of the microcontroller in use.

(3.2)

$$f_{sample} < \frac{1}{9 \cdot \tau_{br}}$$

The relation between buffer capacitor C_b , sampling frequency f_{sample} and sensor bandwidth $f_{rotation}$ is shown in **Figure 12**. In this calculation, sensor bandwidth $f_{rotation}$ is calculated assuming that the phase shift Φ between external magnetic field and electrical sine/cosine output signal is less than 0.2° according to **Equation (2.5)**. R_{TMR} is assumed to be $8\text{k}\Omega$.

Connection to a micro controller

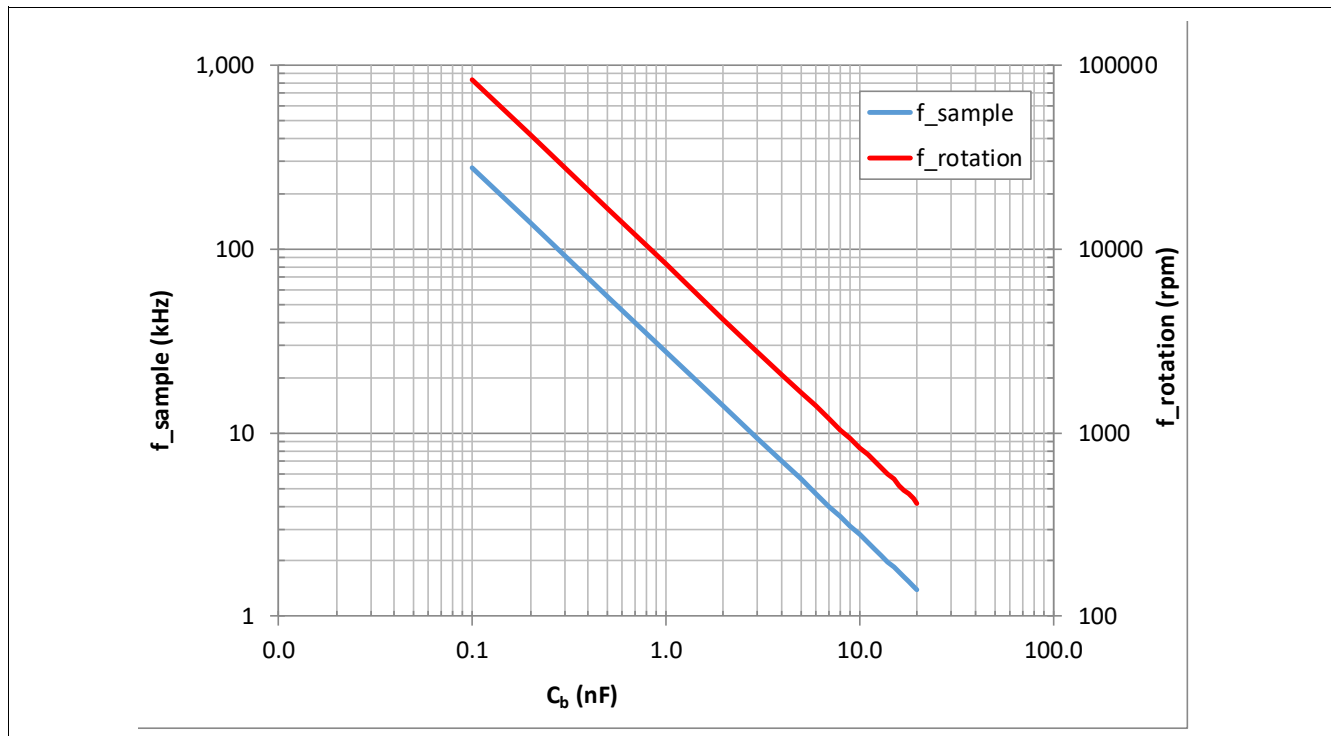


Figure 12 Sampling frequency f_{sample} and sensor bandwidth f_{rotation} as function of the buffer capacitor C_b . R_{TMR} is assumed to be $8k\Omega$.

3.2.2 Load step reduction

As seen in [Equation \(3.1\)](#), the drop of the voltage at the start of the ADC sampling (closing of S/H switch) can be reduced by increasing the value of C_b . If this load step ΔU is less than 0.5 LSB, it is no longer visible and there is no need for a dedicated waiting time until the signal settles. Using [Equation \(3.1\)](#) the following relation can be obtained (N: bits of the ADC):

(3.3)

$$C_b > (2^{N+1} - 1) \cdot C_{\text{SH}}$$

For a 12bit ADC and $C_{\text{SH}} = 7\text{pF}$, the buffer capacitor C_b has to be larger than 57.3nF. In this case, the voltage drop during ADC sampling is less than 0.5 LSB and therefore not visible.

On the other side, such a large buffer capacitor limits the bandwidth of the sensor and the time constant of the bridge calculates to $\tau_{\text{br}} = 229.3\mu\text{s}$. For the phase shift to be less than 0.2° , the maximum frequency of the applied magnetic field f_{rotation} has to be below 145rpm according to [Equation \(2.5\)](#).

In this approach, the sampling frequency can be increased but the bandwidth of the sensor is reduced at the same time.

For a specific application, the best combination of required bandwidth, sampling frequency and sampling accuracy has to be found and the buffer capacitor C_b has to be selected accordingly.

Connection to a micro controller

3.2.3 Oversampling

As seen in [Chapter 3.2.1](#) the sampling frequency f_{sample} is mainly given by the buffer capacitor C_b . In some cases, it might be necessary to perform an oversampling, i.e. to measure the same value several times and calculate the average to increase resolution. [Figure 13](#) shows an extreme condition with $C_b = 1\text{nF}$, a sampling time of $1\mu\text{s}$ and a hold time of $1\mu\text{s}$, giving a total conversion time of $2\mu\text{s}$. In this case the buffer capacitor C_b is not full charged as the time constant of the bridge is much larger than the sampling time. After each sampling step, the voltage drops further and can not fully recover in the following hold time.

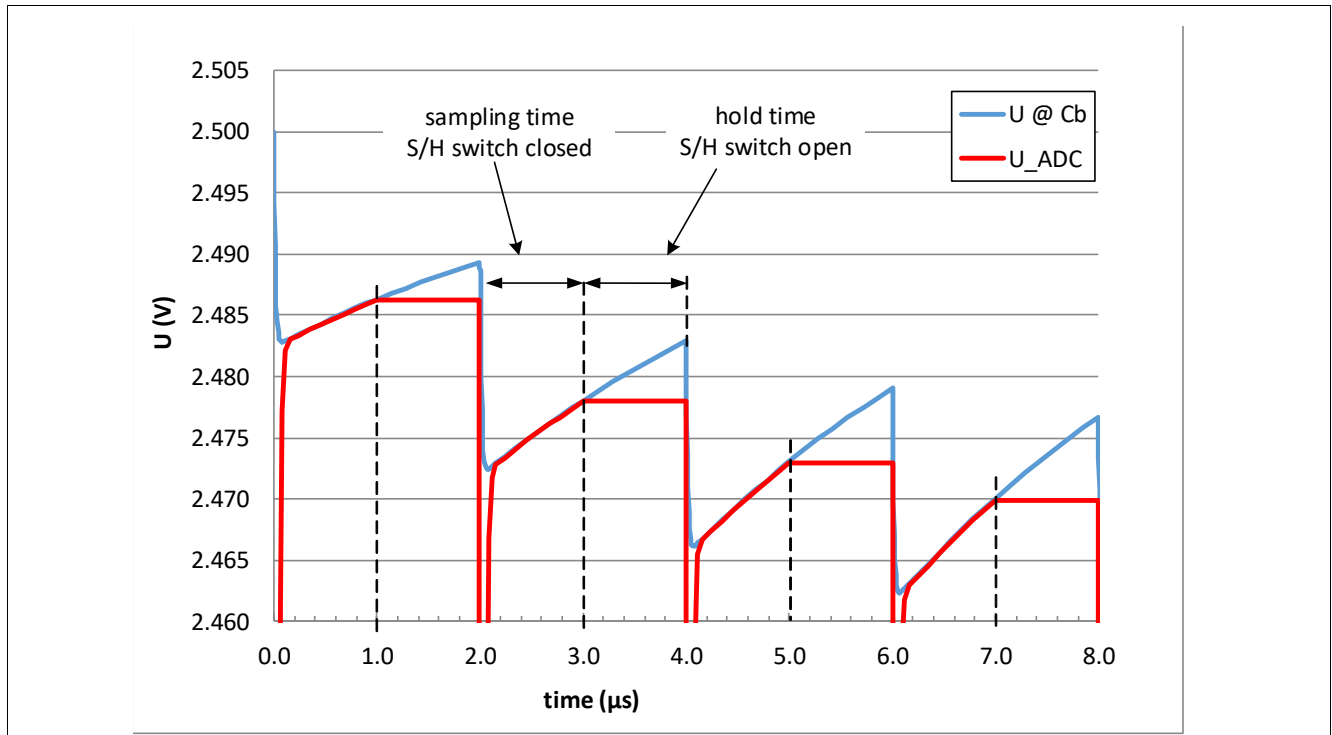


Figure 13 ADC voltage for a sampling time of $1\mu\text{s}$ and a conversion time of $1\mu\text{s}$

As a consequence, the measured sine and cosine output voltage has an error which can contribute to an additional angle error. As long as it is a constant and stable condition, this amplitude error is compensated when doing the sensor calibration (matching of sine and cosine amplitude). Furthermore, as only the ratio of sine and cosine amplitude is relevant for the angle calculation, a part of this error is canceled.

Nevertheless, the user has to verify in the specific application, whether the selected oversampling parameters (sampling time and hold time), together with the external circuitry meets the requirements in angle accuracy.

4 Calibration

Before the TLE5501 can be used in an application, a calibration on system level has to be performed. The four analog output signals SIN_P, SIN_N, COS_P, COS_N have usually an offset and an amplitude mismatch. This has to be corrected before the angle can be calculated. Also, SIN and COS output signals have an orthogonality error, means that they are not precisely 90° phase shifted. This needs also to be compensated to achieve the accuracy specified in the datasheet. The calibration has to be done for all single ended signals which are intended to be used. In case the differential signals are used, there must also be a compensation based on the differential signals. Further details how to perform the calibration is described in the Application Note “**TLE5xxx(D)_Calibration_360**”. Usually this calibration is performed at 25°C and at 0h.

The sensor TLE5501 is intended to be used with a specified magnetic field strength, which range is specified in the datasheet. It has to be ensured that the device is not exposed to a magnetic field outside the specified range over the whole temperature and lifetime range. Also the temperature characteristics of the magnet in use has to be considered. For the usual magnet material, the magnetic field strength is reduced with increasing temperature and increased with decreasing temperature. Therefore, depending on the maximum and minimum temperatures in the application, the magnetic field at 25°C and 0h has to be adjusted accordingly in order not to violate the specified limits. Given a specified range of 25mT to 80mT for the allowed magnetic field range and considering a ferrite magnet material with $T_c = -2000\text{ppm/K}$, the magnetic field in the whole temperature range will be as shown as in **Figure 14**.

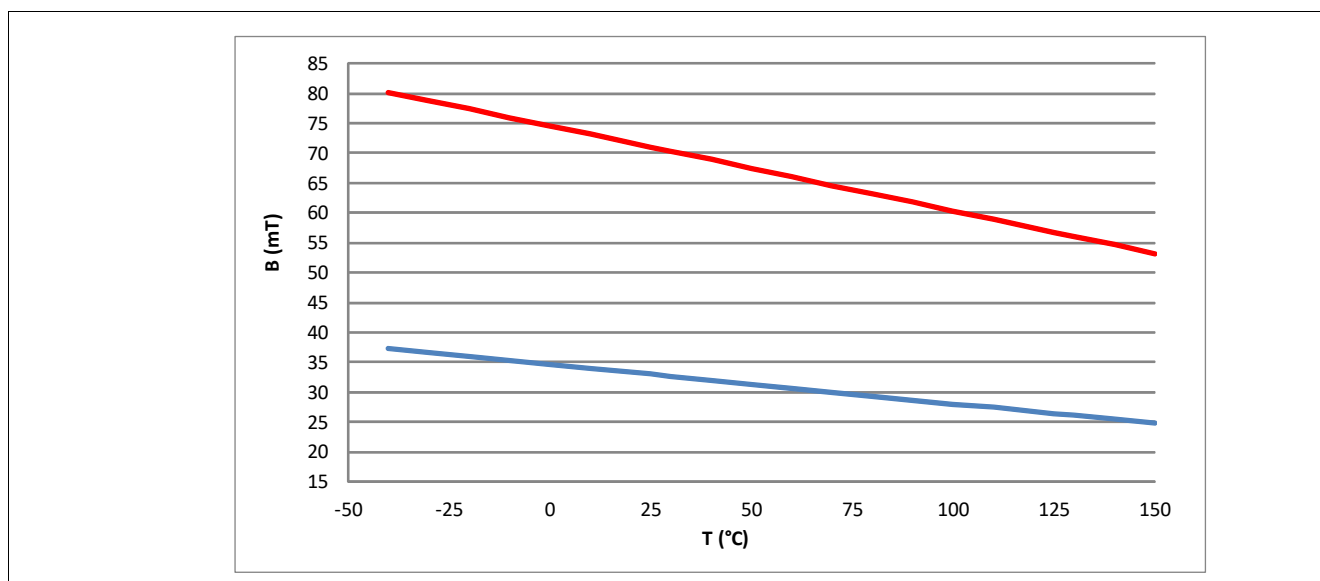


Figure 14 Magnetic field for a ferrite magnet with $TC = -2000\text{ppm/K}$ in the full temperature range. Specified minimum and maximum field values of 25mT and 80mT are considered.

Different magnet material leads to a different temperature characteristic of the magnetic field. This has to be taken into account by the user of the device.

To achieve the specified angle accuracy of TLE5501, it has to be ensured that the magnetic field during lifetime and temperature range of the application does not deviate too much from the initial calibration condition at 25°C/ B_0 /0h. B_0 is the magnetic field at initial calibration condition at 25°C/0h.

This condition is met when the deviation of B_0 over lifetime (due to e.g. aging of magnet and mechanical airgap variations) is less than 10%.

Calibration

Therefore, the following relation has to be ensured by the user over the complete lifetime:

$$B_{\min} = 0.9B_0 < B < 1.1B_0 = B_{\max} ; \text{ with } B_0: \text{ magnetic field at } 25^\circ\text{C}/0\text{h} \text{ and } B_{\min}, B_{\max}: \text{ minimum and maximum magnetic field at initial calibration condition (} 25^\circ\text{C) over lifetime}$$

The temperature behavior of B_{\min} and B_{\max} is given by the temperature coefficient of the magnet material. An example for an initial calibration point at $25^\circ\text{C}/50\text{mT}/0\text{h}$ is shown in **Figure 15**.

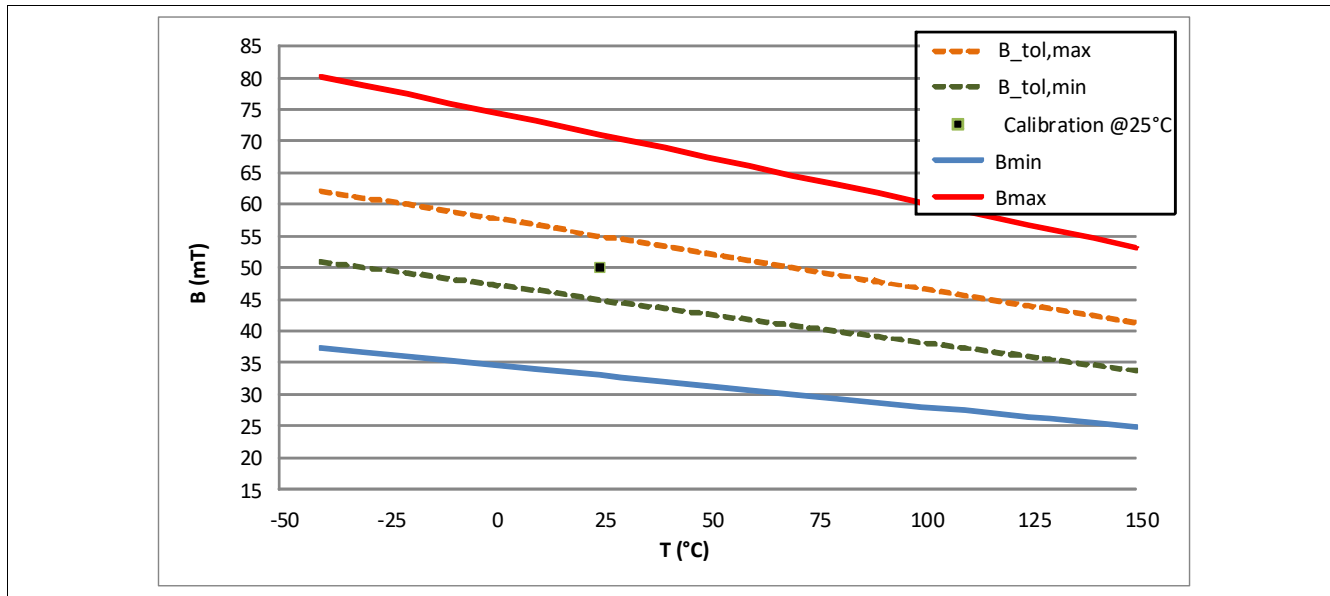


Figure 15 One-time calibration a $25^\circ\text{C}/50\text{mT}$. Dashed lines show the allowed magnetic field range taking into account the temperature effect and aging of the magnet. Assumptions: ferrite magnet material with $\text{TC} = -2000\text{ppm/K}$, 10% field strength variation from initial calibration condition ($25^\circ\text{C}/50\text{mT}$) over lifetime.

Figure 16 shows the typical angle error for a sensor which has its initial calibration of offset, amplitude and orthogonality error at $25^\circ\text{C}/50\text{mT}$. Due to aging effects of the magnet, it is assumed that the magnetic field at 25°C is reduced by 10% to 45mT . The sensor is still operated with calibration parameters coming from initial calibration at $25^\circ\text{C}/50\text{mT}$, thus having no longer optimized calibration values. Over temperature, the magnetic field is changing with a T_c of -2000ppm/K (ferrite magnet material is assumed). This means that the magnetic field at the sensor deviates more or less (depending on temperature) from the initial calibration condition $B_0 = 50\text{mT}$. This deviation causes an angle error which is shown in **Figure 16**.

Calibration

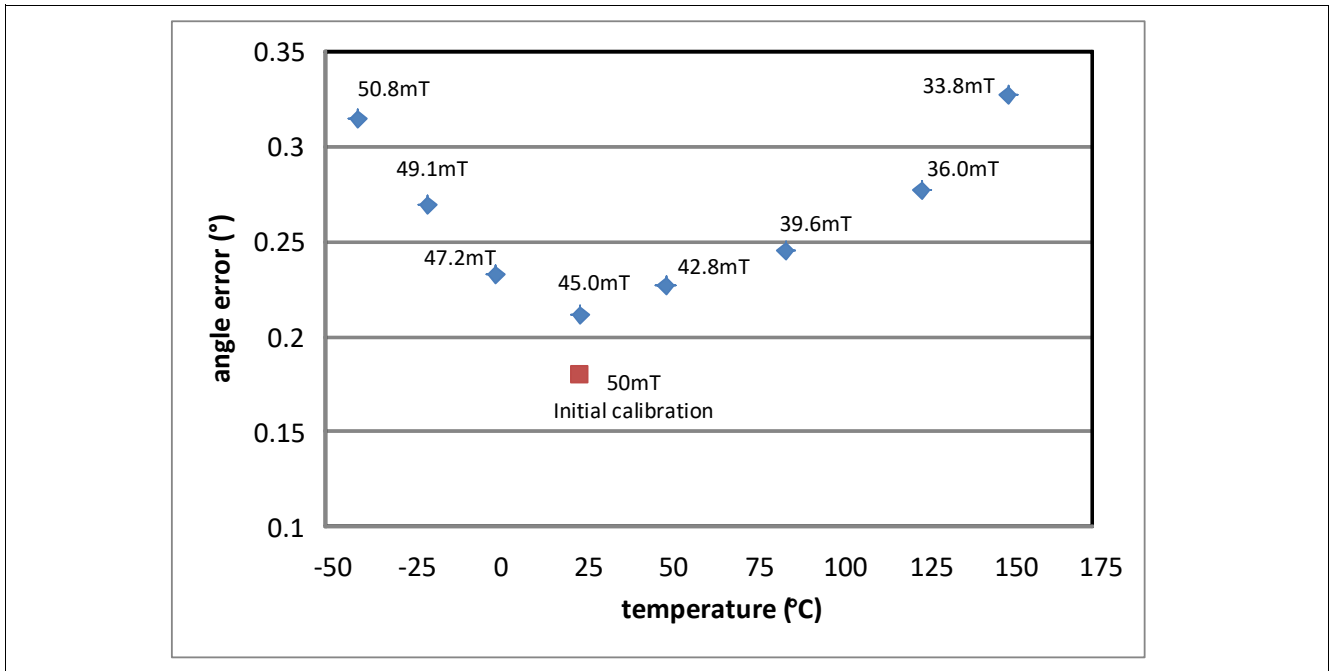


Figure 16 Typical angle error with initial calibration at 25°C/50mT and subsequent measurements considering 10% magnetic field change due to aging and air gap variation (i.e. 45mT @25°C). Magnetic field values change with a TC of -2000ppm/K (ferrite magnet material). Magnetic field values are indicated at each measurement temperature.

Revision History

5 Revision History

Revision	Date	Changes
0.1	2019-04-29	Initial version

Trademarks of Infineon Technologies AG

All referenced product or service names and trademarks are the property of their respective owners.

Edition 2019-04-29

Published by

Infineon Technologies AG

81726 Munich, Germany

© 2019 Infineon Technologies AG.

All Rights Reserved.

Do you have a question about any aspect of this document?

Email: erratum@infineon.com

Document reference

IMPORTANT NOTICE

The information contained in this application note is given as a hint for the implementation of the product only and shall in no event be regarded as a description or warranty of a certain functionality, condition or quality of the product. Before implementation of the product, the recipient of this application note must verify any function and other technical information given herein in the real application. Infineon Technologies hereby disclaims any and all warranties and liabilities of any kind (including without limitation warranties of non-infringement of intellectual property rights of any third party) with respect to any and all information given in this application note.

The data contained in this document is exclusively intended for technically trained staff. It is the responsibility of customer's technical departments to evaluate the suitability of the product for the intended application and the completeness of the product information given in this document with respect to such application.

For further information on technology, delivery terms and conditions and prices, please contact the nearest Infineon Technologies Office (www.infineon.com).

WARNINGS

Due to technical requirements products may contain dangerous substances. For information on the types in question please contact your nearest Infineon Technologies office.

Except as otherwise explicitly approved by Infineon Technologies in a written document signed by authorized representatives of Infineon Technologies, Infineon Technologies' products may not be used in any applications where a failure of the product or any consequences of the use thereof can reasonably be expected to result in personal injury.